Thermo-mechanical adjustment after impacts during planetary growth

Julien Monteux, Nicolas Coltice, Fabien Dubuffet, Yanick Ricard

Thermo-mechanical adjustment after impacts during planetary growth

Julien Monteux,[1] Nicolas Coltice,[1] Fabien Dubuffet,[1] and Yanick Ricard[1]

Received 29 August 2007; accepted 7 November 2007; published 18 December 2007.

[1] The thermal evolution of planets during their growth is strongly influenced by impact heating. The temperature increase after a collision is mostly located next to the shock. For Moon to Mars size planets where impact melting is limited, the long term thermo-mechanical readjustment is driven by spreading and cooling of the heated zone. To determine the time and length scales of the adjustment, we developed a numerical model in axisymmetric cylindrical geometry with variable viscosity. We show that if the impactor is larger than a critical size, the spherical heated zone isothermally flattens until its thickness reaches a value for which motionless thermal diffusion becomes more effective. The thickness at the end of advection depends only on the physical properties of the impacted body. The obtained timescales for the adjustment are comparable to the duration of planetary accretion and depend mostly on the physical properties of the impacted body. **Citation:** Monteux, J., N. Coltice, F. Dubuffet, and Y. Ricard (2007), Thermo-mechanical adjustment after impacts during planetary growth, *Geophys. Res. Lett.*, *34*, L24201, doi:10.1029/2007GL031635.

1. Introduction

[2] Impacts have strongly influenced the evolution of planets: a collision of the Earth with a Mars-sized body is at the origin of the formation of the Moon [*Hartmann and Davis*, 1975] and the impact by a kilometer-sized body could be responsible for the mass extinction at the K-T boundary [*Alvarez et al.*, 1980]. It is during accretion that impacts played the most significant role, depositing and burying heat into growing planetary bodies.

[3] When the impact velocity becomes larger than the elastic velocities, a shock wave develops. The shock pressure, increasing with the size of the impacted body, is nearly uniform in a spherical region next to the impact (the isobaric core), and strongly decays away from it [*Croft*, 1982]. Following the adiabatic pressure release, the peak pressure being independent of impactor size, a temperature increase of several hundred degrees remains on Moon to Mars size bodies [*Senshu et al.*, 2002] (see equation (2)). Hence, the hotter temperatures are located close to the surface during planetary growth [*Kaula*, 1979] and large impacts have caused extensive melting and formation of magma oceans on Earth [*Tonks and Melosh*, 1993].

[4] The thermal anomaly caused by an impact generates a buoyant thermal anomaly that ultimately drives an isostatic adjustment. If the impact velocity is larger than 7.5 km.s^{-1}, a significant volume of the isobaric core is molten [*O'Keefe and Ahrens*, 1977] hence the adjustment is controlled by two-phase flow and probably hydrofracturation [*Solomatov*, 2000]. For smaller planets or planetesimals, melting is nearly absent therefore the thermo-mechanical adjustment is dominated by the slow viscous deformation and thermal diffusion of the hot thermal anomaly.

[5] In this study, we investigate the thermal relaxation and viscous deformation after the shock of an impactor on a small planet or planetesimal in order to derive scalings for the relevant length and time scales of the thermo-mechanical adjustment.

2. Model Description

2.1. Thermal State After an Impact

[6] Energy balance calculations and shock simulations suggest that the radius of the isobaric core R_{ic} is comparable or slightly larger than that of the impactor R_{imp} and we use $R_{ic} = 3^{1/3} R_{imp}$ [*Senshu et al.*, 2002; *Pierazzo et al.*, 1997]. Away from the isobaric core, the shock wave propagates and the peak pressure decays with the square of the distance r from the center of the isobaric core [*Pierazzo et al.*, 1997]. Just after the adiabatic pressure release, the thermal perturbation corresponds to an isothermal sphere of radius R_{ic} and temperature $T_0 + \Delta T$ that decays when $r > R_{ic}$ as

$$T(r) = T_0 + \Delta T \left(\frac{R_{ic}}{r}\right)^m, \quad (1)$$

with $m \sim 4.4$ as proposed by *Senshu et al.* [2002].

[7] The energy dissipated as heat following the shock is a fraction of the kinetic energy of the impactor. The impactor velocity v_{imp} should be comparable to the escape velocity $v_{imp} = \sqrt{2gR}$, where $g = 4/3\ G\pi\rho R$, ρ and R are the gravity, density and radius of the impacted growing planet [*Kokubo and Ida*, 1996]. Assuming $\rho \sim \rho_{imp} \sim \rho_{ic}$, the temperature increase ΔT is

$$\Delta T = \frac{4\pi}{9} \frac{\gamma}{f(m)} \frac{\rho G R^2}{C_p}, \quad (2)$$

where C_p is the heat capacity of the impacted body and G is the gravitational constant. The efficiency of kinetic to thermal energy conversion γ is close to 0.3 according to physical and numerical models [*O'Keefe and Ahrens*, 1977]. The function $f(m)$ represents the volume effectively heated normalized by the volume of the isobaric core (i.e., $f(m) = 1$ if only the isobaric core is heated). Assuming $R_{ic} \ll R$ and integrating equation (1) leads to $f(m) \sim 2.7$ and 37% of the impact heating is released within the isobaric core. The temperature increase does not depend on the size of the impactor but on the square of the radius of the impacted body.

[1] Laboratoire de Sciences de la Terre, UMR 5570, CNRS, Université de Lyon, Université Claude Bernard Lyon 1, Ecole Normale Supérieure de Lyon, Villeurbanne, France.

0094-8276/07/2007GL031635$05.00

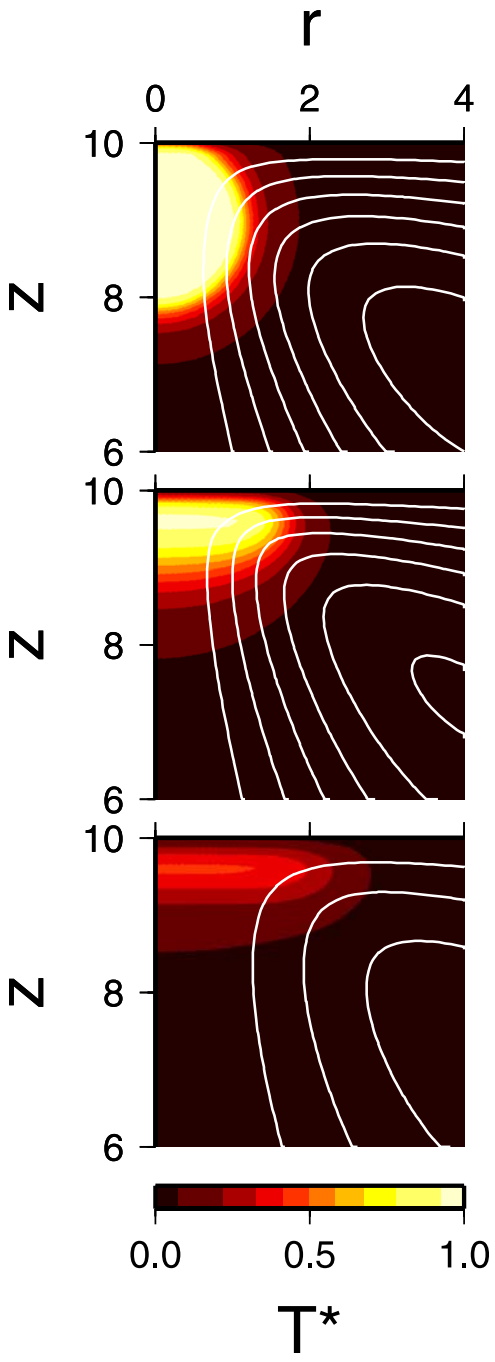

Figure 1. Close up view of the non dimensional temperature fields and streamlines computed for a temperature dependent viscosity at non-dimensionalized times (top) $t^* = 0$, (middle) $t^* = 3$ and (bottom) $t^* = 10$ (we use $\lambda = 10^{-2}$ and $Ra_{ic} = 10^2$ (see 2.2)).

[8] Immediately after the shock, a fraction of the isobaric core is removed during crater excavation. However, it is only for small impactors (less than 5 km of radius) and large planets (more than 3000 km of radius) that a significant fraction of the heated zone is redistributed [*Maxwell*, 1977]. Because our study is focused on large impacts (>10km) on small planets (<3000km), we can neglect the excavated heat or consider it as an additional uncertainty on the parameters γ or $f(m)$ (see equation (2)). Following excavation, reduction of the crater depth to at most few kilometers takes place through isostatic rebound. The total amount of vertical motion that occurs during the isostatic process (a few km), and its duration (typically a few 10^3y) are negligible compared to the length scales and timescales of thermal readjustment. After the crater formation, most of the initial energy still remains below the crater [*Turtle et al.*, 2003]. Modelling these processes of mass and energy redistribution is beyond the scope of this paper since we are interested in the long term consequences of shock heating as in work by *Reese et al.* [2002].

[9] The proposed thermal state following an impact sketched in Figure 1 (top) is that of a cold body of homogeneous temperature T_0 perturbed by the impact of a sphere of radius R_{ic} (the depth of the crater being negligible compared to the heated zone).

2.2. Thermo-Mechanical Model

[10] The governing non-dimensional equations for the extremely viscous flow of a cooling hot drop are

$$-\vec{\nabla}P^* + \vec{\nabla}.\left(\frac{\eta(T^*)}{\eta_0}\vec{\nabla}\vec{v}^* + \left[\frac{\eta(T^*)}{\eta_0}\vec{\nabla}\vec{v}^*\right]^T\right) + T^*\vec{e}_z = 0, \tag{3}$$

$$\frac{\partial T^*}{\partial t^*} = \frac{\nabla^2 T^*}{Ra_{ic}} - \vec{v}^*.\vec{\nabla}T^*, \tag{4}$$

$$\vec{\nabla}.\ \vec{v}^* = 0, \tag{5}$$

where distances, temperature and velocity are normalized by R_{ic}, ΔT and the characteristic Stokes velocity v_s of the isobaric core

$$v_s = \frac{\alpha\rho g\Delta T R_{ic}^2}{\eta_0}, \tag{6}$$

where η_0 is the viscosity far from the impact and α the thermal expansivity of the impacted body. Ra_{ic} is the Rayleigh number based on the isobaric core radius:

$$Ra_{ic} = \frac{\alpha\rho g\Delta T R_{ic}^3}{\kappa\eta_0}. \tag{7}$$

We define a Rayleigh number based on the size of the isobaric core R_{ic} since in all our experiments, the radius of the planet R remains much larger than R_{ic} and thus does not affect the dynamics except through the gravity and the temperature increase (see equation (2)).

[11] For planets of Moon to Mars size the gravity and the temperature increase are not very large (e.g. $g \simeq 3$ m s^{-2}, $\Delta T \simeq 300$ K). We also consider impactors with radius small compared to the planet radius (e.g. $R_{ic} \simeq 300$ km). In this case, Ra_{ic} should remain moderate (say lower than 10^5) assuming that the coldest material of the growing planetesimal have a viscosity η_0 comparable to that of the present day Earth, say around 10^{21} Pa s (e.g. $Ra_{ic} \simeq 4700$ for $\kappa = 10^{-6}$ m^{2}s^{-1}, $\alpha = 5 \times 10^{-5}$ K^{-1}, $C_p = 1200$ J K^{-1} kg^{-1}, $\rho = 3870$ kg m^{-3}). The viscosity is temperature-dependent

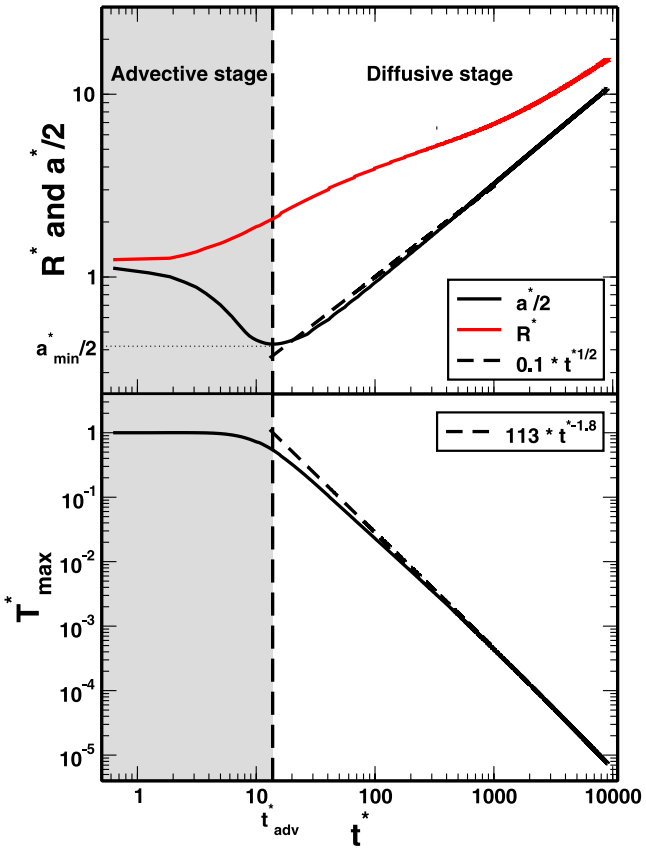

Figure 2. (top) Thickness $a^*/2$ (black solid line) and radial extent R^* (red solid line) and (bottom) maximal temperature at $r = 0$ as functions of time t^* for $Ra_{ic} = 10^2$. Power-law fits following a diffusive solution are depicted by dashed lines. The equilibrium between diffusive (gray field) and advective (white field) stages is obtained at $t^* = t^*_{adv}$.

$\eta(T^*) = \eta_0 \lambda^{T^*}$, λ being the viscosity ratio (lower than 1) between the hottest ($T^* = 1$) and the coldest ($T^* = 0$) material. This viscosity decreases sharply with temperature and its expression is simpler to implement than the usual Arrhenius law.

[12] We developed and benchmarked against analytical solutions a finite difference code to solve equations (3) and (5) in axisymmetric cylindrical geometry. We use a stream function formulation for the Stokes equation with a direct implicit inversion method [*Schubert et al.*, 2001]. The heat equation (4) is solved by an Alternating Direction Implicit (ADI) scheme. All the equations are discretized with a second order accuracy in space and time. Advection terms are calculated with a centered differences scheme. This scheme is known to produce numerical oscillations for grid Peclet numbers larger than $\simeq$20 (the grid Peclet number is $Ra\Delta x^2 v^*/\Delta t$ where Δx is the grid dimension and Δt the time step) [*Dubuffet et al.*, 2000] but in our simulations, the maximum Peclet number remains of order unity. We used at least 129 $\times$ 129 grid points and the dimensions of the calculation domain varies between $10R_{ic} \times 10R_{ic}$ and $100R_{ic} \times 100R_{ic}$. Boundary conditions are free-slip, isothermal at the surface and insulating on other walls. In order to keep a good accuracy in a large enough domain and with strong viscosity variations we run the simulations up to $Ra_{ic} = 10^4$ only, from which we fit scaling laws that can be extrapolated to higher Rayleigh numbers.

[13] The geometrical evolution of the post-impact thermal anomaly as a function of time is monitored by its nondimensional radial extent $R^*(t^*)$, its thickness $a^*(t^*)$ and its maximum temperature $T^*_{\max}(t^*)$. $a^*(t^*)$ is the depth where the second derivative of the vertical temperature profile at $r^* = 0$ is zero. Along this profile the maximum temperature value $T^*_{\max}(t^*)$ is reached at $z^* = z^*_{\max}$. $R^*(t^*)$ is the distance where the second derivative of the horizontal temperature profile at $z^* = z^*_{\max}$ is zero.

3. Results

[14] For large enough Rayleigh numbers, the thermal relaxation consists in an early advective stage corresponding to an isothermal flattening of the hot drop, followed by a later stage of diffusive cooling. For $Ra_{ic} \leq 4.9$, cooling is motionless.

3.1. Advective Stage and Diffusive Stage

[15] Figure 2 shows a first stage in the thermal relaxation corresponding to isothermal spreading of the buoyant hot region below the surface. This phenomenon of viscous gravity currents has been widely studied [*Bercovici and Lin*, 1996; *Koch and Koch*, 1995; *Huppert*, 1982; *Koch and Manga*, 1996]. The evolution of the shape is comparable to these works even though they were either designed to study mantle plumes fed by a deeper conduit [*Bercovici and Lin*, 1996] or compositional plumes [*Koch and Manga*, 1996]. Moreover, the analytical results and scaling laws given by *Koch and Koch* [1995] have been mostly derived in a regime where $R^* \gg a^*$ which is not really the case in our calculations.

[16] During the advective stage (see Figure 1 (middle)), the aspect ratio of the drop is increasing while the temperature and the volume of the thermal anomaly remain nearly constant, i.e.

$$\frac{a^*}{2} R^* 2 \sim 1. \tag{8}$$

The second stage of thermal relaxation is dominated by diffusion. After the hot drop stops flattening, heat is diffused in all directions and more efficiently through the top isothermal cold surface. As a consequence, R^* and a^* increase with time as seen in Figure 2. The evolution of $a^*(t^*)$ is rapidly consistent with a purely diffusive model: $a^*(t^*) \sim \sqrt{2\kappa t^*}$. The lateral extent, $R^*(t^*)$, evolves more slowly but reaches a similar diffusive behavior after a long time. The temperature decreases rapidly with the power of -1.8 (see Figure 1 (bottom) and Figure 2).

3.2. Time and Length Scales

[17] The transition from the advective to the diffusive stage happens when the diffusion velocity, κ/a overcomes the advection velocity which is of order $\alpha\rho g \Delta T a^2/\eta_0$. This simple balance implies that

$$\frac{a^*_{\min}}{2} = c_1 Ra_{ic}^{-1/3}, \tag{9}$$

where c_1 is a constant. The volume of the hot anomaly being constant, the radius of the thermal anomaly at the end

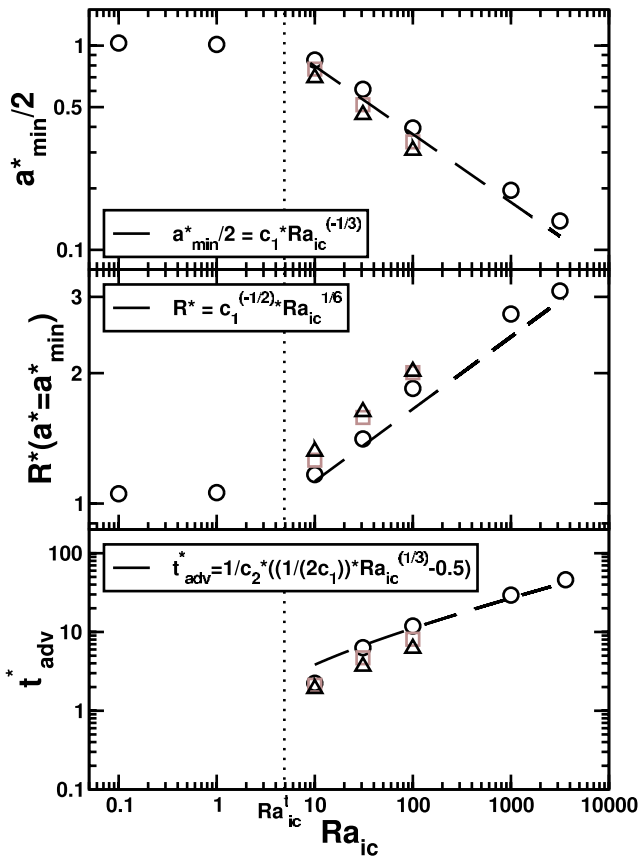

Figure 3. (top) Minimum thickness $a^*_{\min}/2$, (middle) radial extent R^* and (bottom) time of equilibrium t^*_{adv} as functions of Ra_{ic} for different viscosity contrasts (black circles for a uniform viscosity, brown squares and black triangles for $\lambda = 10^{-1}$ and $\lambda = 10^{-2}$). The dashed lines correspond to the predictions of equations (9),(10), and (12) (we use $c_1 = 1.7$, $c_2 = 0.2$).

of the advective stage, R^*_{adv} is easily obtained by combining equations (8) and (9):

$$R^*_{adv} = {c_1}^{-1/2} Ra_{ic}^{1/6}. \tag{10}$$

[18] The time t_{adv} at the end of the advection stage corresponds to the time needed to advect the bottom of the thermal anomal from its initial depth $2R_{ic}$ to its final depth $a_{\min}$. As the vertical velocity $\partial a/\partial t$ is of order of $-\alpha\rho g\Delta T a^2/\eta_0$, we get

$$\frac{\partial a}{\partial t} = -c_2 \frac{\alpha\rho g \Delta T a^2}{\eta_0}, \tag{11}$$

where c_2 is a geometrical factor.

[19] Integration of equation (11) from $a(0) = 2R_{ic}$ to $a(t_{adv}) = a_{\min}$ using equation (9) implies that the end of the advection phase occurs at

$$t^*_{adv} = \frac{1}{c_2}\left(\frac{1}{2c_1} Ra_{ic}^{1/3} - \frac{1}{2}\right). \tag{12}$$

[20] These scalings of equations (9), (10), and (12) are confirmed by fitting the results of the numerical experiments shown in Figure 3 with $c_1 \sim 1.7$ and $c_2 \sim 0.2$.

[21] Of course, the transition between advective and diffusive stages only occurs when the initial size of the isobaric core is larger than the minimum thickness given by equation (9). This threshold R^t_{ic} obtained when $a^*_{\min} = 2$ corresponds to the threshold Rayleigh number

$$Ra^t_{ic} = c_1^3 = 4.9. \tag{13}$$

For $Ra_{ic} < Ra^t_{ic}$, $a^*_{\min} = 2R_{ic}$ and t^*_{adv} is not defined. Below Ra^t_{ic} the heat is diffused out without advection.

[22] The previous scalings obtained for a uniform viscosity are also valid for large viscosity contrasts. Our simulations depicted in Figure 3 (squares for $\lambda = 10^{-1}$ and triangles for $\lambda = 10^{-2}$) show that large viscosity contrasts enable the drop an easier spreading below the surface in agreement with *Koch and Koch* [1995]. As the resistance to internal shearing decreases with λ, horizontal velocity contrasts are more important for low viscosities. As a result, the thickness decreases by about 10%, the radial extent increases by a similar amount and the advection time decreases by a factor ~2. The temperature dependence of the viscosity affects our results by a minor amount because the readjustment is mostly controlled by the viscosity far from the isobaric core.

[23] The scaling laws with physical dimensions can be easily expressed. Using equation (2) and assuming that the planet density remains uniform so that $g = 4/3\pi G\rho R$, the minimal thickness of the thermal anomaly and the time to reach this thickness are

$$a_{\min} = 2b_1 \frac{L^2}{R} \tag{14}$$

and

$$t_{adv} = b_2 \frac{L^2}{\kappa}\left(\frac{L}{R}\right)^2\left(1 - b_1 \frac{L^2}{RR_{ic}}\right). \tag{15}$$

In these expressions, b_1 and b_2 are dimensionless constants,

$$b_1 = \frac{3}{2} c_1 \left(\frac{f(m)}{2\gamma\pi^2}\right)^{1/3} \sim 1.96, \qquad b_2 = \frac{b_1^2}{2c_1^3 c_2} \sim 1.96, \tag{16}$$

and the properties of the impacted planet appear through a characteristic length

$$L = \left(\frac{C_p \kappa \eta_0}{\alpha\rho^3 G^2}\right)^{1/6} \sim 212 \text{ km}. \tag{17}$$

4. Discussion and Conclusion

[24] We developed a thermo-mechanical model for the long term relaxation after an impact. In a first stage, the heated region spreads below the surface until diffusive cooling becomes more effective. The transition between the advective and diffusive stages is described by a thickness $a_{\min}$ and timescale t_{adv} for which we proposed scalings

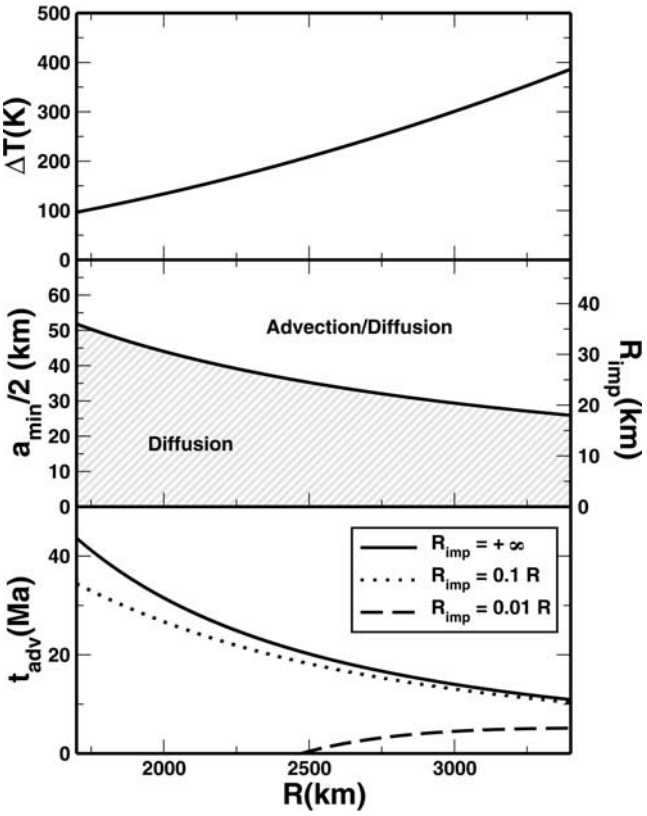

Figure 4. (top) Temperature increase ΔT, (middle) thickness $a_{\min}/2$ and (bottom) advection time t_{adv} as functions of the planetary radius. For too small impactors (right side label), advection does not occur. The advection time is plotted for different impactor radii.

laws. Hence we can predict geometrical and time evolution of the thermal anomaly caused by a meteoritical impact as functions of rheological parameters of the impacted planetesimal and impactor. All our results are summarized in Figure 4.

[25] The temperature increase (Figure 4, top) and the thickness of the thermal anomaly after advection (Figure 4, middle) do not depend on the initial size of the impactor but only on the properties of the impacted body (and therefore its radius assuming known its other properties, see equations (2) and (14)). As the volume of the isobaric core is proportional to that of the impactor the minimum thickness of the thermal anomaly corresponds also to the minimum radius of the impactor that can trigger advection (Figure 4, middle). For a Mars size planet (R = 3400 km), impacts increase the temperature by 390 K (in relative agreement with *Senshu et al.* [2002]) and post-impact advection only occurs for impactors with radius larger than 18 km. After advection, the final thickness of the thermal anomaly is 52 km. For smaller impactors, only heat diffusion occurs.

[26] The duration of advection depends on the impactor size (Figure 4, bottom). As shown in equation (15), the time of advection is lower than a threshold value obtained for an infinitely large impactor (which of course would disrupt the planet). For a Mars size planet impacted by bodies with 1/10 to 1/100 smaller radii, advection ends up after, 10 Myr, 5 Myr, respectively. After this advective stage, heat is slowly removed by diffusion in ~20 Myr.

[27] These timescales are of the same order as those for accretion and differentiation [*Yin et al.*, 2002]. Hence, until impact melting is efficient, heat brought by impacts is stored within the mantle even taking into account of the deformation of the heated region. The scalings proposed here could be used to compute more accurate one dimensional thermal evolution models of growing planets.

[28] **Acknowledgments.** The authors thank J. Schmalzl, H. Samuel and an anonymous reviewer for their useful comments about the manuscript. They also thank J. Melosh and M. Monnereau for helpful discussions. This project was funded by the A.N.R. ETHER.

References

Alvarez, L. W., W. Alvarez, F. Asaro, and H. V. Michel (1980), Extraterrestrial cause for the Cretaceous Tertiary extinction, *Science*, *208*, 1095–1108.

Bercovici, D., and J. Lin (1996), A gravity current model of cooling mantle plume heads with temperature-dependent buoyancy and viscosity, *J. Geophys. Res.*, *101*, 3291–3310.

Croft, S. K. (1982), A first-order estimate of shock heating and vaporization in oceanic impacts, in *Geological Implications of Impacts of Large Asteroids and Comets on Earth*, edited by T. L. Silver and P. H. Schultz, *Spec. Pap. Geol. Soc. Am.*, *90*, 143–152.

Dubuffet, F., M. Rabinowicz, and M. Monnereau (2000), Multiple scales in mantle convection, *Earth Planet. Sci. Lett.*, *178*, 351–366.

Hartmann, W. K., and D. R. Davis (1975), Satellite-sized planetesimals and lunar origin, *Icarus*, *24*, 504–514.

Huppert, H. E. (1982), The propagation of two-dimensional and axisymmetric viscous gravity currents over a rigid horizontal surface, *J. Fluid Mech.*, *121*, 43–58.

Kaula, W. M. (1979), Thermal evolution of Earth and Moon growing by planetesimal impacts, *J. Geophys. Res.*, *84*, 999–1008.

Koch, D. M., and D. L. Koch (1995), Numerical and theoretical solutions for a drop spreading below a free fluid surface, *J. Fluid Mech.*, *287*, 251–278.

Koch, D. M., and M. Manga (1996), Neutrally buoyant diapirs: A model for Venus coronae, *Geophys. Res. Lett.*, *23*, 225–228.

Kokubo, E., and S. Ida (1996), On runaway growth of planetesimals, *Icarus*, *123*, 180–191.

Maxwell, D. E. (1977), Simple Z model for cratering, ejection, and the overturned flap, in *Impact and Explosion Cratering: Planetary and Terrestrial Implications*, edited by D. J. Roddy, R. O. Pepin, and R. B. Merrill, pp. 1003–1008, Elsevier, New York.

O'Keefe, J. D., and T. J. Ahrens (1977), Impact-induced energy partitioning, melting, and vaporization on terrestrial planets, *Lunar Planet. Sci. Conf.*, *8th*, 3357–3374.

Pierazzo, E., A. M. Vickery, and H. J. Melosh (1997), A reevaluation of impact melt production, *Icarus*, 408–423.

Reese, C. C., V. S. Solomatov, and J. R. Baumgardner (2002), Survival of impact-induced thermal anomalies in the Martian mantle, *J. Geophys. Res.*, *107*(E10), 5082, doi:10.1029/2000JE001474.

Schubert, G., D. L. Turcotte, and P. Olson (2001), *Mantle Convection in the Earth and Planets*, Cambridge Univ. Press, New York.

Senshu, H., K. Kuramoto, and T. Matsui (2002), Thermal evolution of a growing Mars, *J. Geophys. Res.*, *107*(E12), 5118, doi:10.1029/2001JE001819.

Solomatov, V. S. (2000), *Fluid Dynamics of a Terrestrial Magma Ocean, Origin of the Earth and Moon*, edited by R. M. Canup et al., pp. 323–338, Univ. of Ariz. Press, Tucson.

Tonks, W. B., and H. J. Melosh (1993), Magma ocean formation due to giant impacts, *J. Geophys. Res.*, *98*, 5319–5333.

Turtle, E. P., E. Pierazzo, and D. P. O'Brien (2003), Numerical modeling of impact heating and cooling of the Vredefort impact structure, *Meteorit. Planet. Sci.*, *38*, 293–303.

Yin, Q., S. B. Jacobsen, K. Yamashita, J. Blichert-Toft, P. Télouk, and F. Albarède (2002), A short timescale for terrestrial planet formation from Hf-W chronometry of meteorites, *Nature*, *418*, 949–952.

N. Coltice, F. Dubuffet, J. Monteux, and Y. Ricard, Laboratoire de Sciences de la Terre, UMR 5570, CNRS, Université de Lyon, Université Claude Bernard Lyon 1, 2 rue R. Dubois, F-69622, Villeurbanne cedex, France. (nicolas.coltice@univ-lyon1.fr; fabien.dubuffet@univ-lyon1.fr; julien.monteux@univ-lyon1.fr; ricard@ens-lyon.fr)